Scaling thermodynamic model for the self-induced nucleation of GaN nanowires

Vladimir G. Dubrovskii,[1,2,3,*] Vincent Consonni,[4,5] Achim Trampert,[4] Lutz Geelhaar,[4] and Henning Riechert[4]

[1]*St. Petersburg Academic University, Khlopina 8/3, 194021 St. Petersburg, Russia*

[2]*Ioffe Physical Technical Institute of the Russian Academy of Sciences, Politekhnicheskaya 26, 194021 St. Petersburg, Russia*

[3]*St. Petersburg State University, Physical Faculty, Peterhof 198904, St. Petersburg, Russia*

[4]*Paul-Drude-Institut für Festkörperelektronik, Hausvogteiplatz 5-7, 10117 Berlin, Germany*

[5]*Laboratoire des Matériaux et du Génie Physique, CNRS–Grenoble INP, 3 parvis Louis Néel, 38016 Grenoble, France*

(Received 8 December 2011; revised manuscript received 3 April 2012; published 23 April 2012; publisher error corrected 1 May 2012)

Self-induced growth of nanowires is a fundamental phenomenon which is qualitatively different from the known growth mechanisms, such as the stress-driven formation of quantum dots or metal-catalyzed vapor-liquid-solid growth of nanowires. We present a scaling thermodynamic model that explains the self-induced nucleation of GaN nanowires by the anisotropy of surface energies coupled with the scaling growth anisotropy. The model shows why GaN tends to nucleate in the form of nanoislands rather than nanowires. It also elucidates the physical origin of the island-to-wire shape transformation at a certain critical radius. It is shown that the self-induced nanowire formation is sensitive to the sidewall surface energy that should be sufficiently low to favor growth anisotropy. The model is in a qualitative agreement with the experimental data and may be applied to other highly anisotropic growths driven by the surface energetics.

DOI: 10.1103/PhysRevB.85.165317 PACS number(s): 68.70.+w, 81.10.Aj

I. INTRODUCTION

Semiconductor nanowires (NWs) are promising building blocks of future nanoelectronic,[1] nanophotonic,[2] and nanosensing[3] devices. The self-induced NW formation is an attractive approach to ease their synthesis and improve functionality. In particular, the self-induced growth of GaN NWs on Si substrates has drawn much attention, since it provides a unique way for the monolithic integration of high-quality GaN nanostructures with a Si platform.[4–20] The self-induced approach is advantageous in many respects. First, it does not require advanced lithography or other sophisticated methods of substrate preparation. Second, self-induced NWs[20] do not suffer from several drawbacks of the vapor-liquid-solid (VLS) NWs, such as crystallographic polytypism[21–23] or Au contamination.[24] As NWs in general, self-induced GaN NWs enable a radical decrease of dislocation density induced by lattice mismatch.[13,16,25,26] That is why the NW geometry is excellent for the formation of optical Ga(In)N/Al(Ga)N heterostructures.[1,2,25,27] The controlled synthesis of self-induced NWs requires, however, a deep understanding of their growth mechanisms, and the initial nucleation step in particular.

There have been a number of important investigations into the fundamentals of self-induced growth. Among these, we mention the studies of GaN NW nucleation on Si substrates, either covered with a crystalline AlN lattice-mismatched layer (hereafter referred to as LML)[13,16,18] or with a Si_xN_y amorphous interlayer (AL),[17,19] the NW growth chronology,[13,15] and the dependence of NW growth rate on different parameters.[7,8,15] Several theoretical approaches have been used to explain the experimentally observed phenomena. They consider, in particular, the strain-induced effects,[16,26] the anisotropy of surface energies,[16,17] and the NW growth models[7,8,15] developed earlier for the VLS NWs.[28] However, none of those approaches is capable of a complete description of the initial NW nucleation stage that should be driven by the energetic factors. In this paper, we try to fill the gap by presenting a quasiequilibrium scaling model qualitatively explaining some important experimentally observed facts. We use a thermodynamic approach[29–31] where the preferred growth configuration corresponds to the minimum formation enthalpy for different geometries. The model might also be useful for a better understanding of self-induced growth of other elongated structures (III-V and II-VI NWs, metal whiskers, etc.), as it reveals general conditions necessary to observe such a growth in a given material system.

Let us now summarize the most important points regarding the self-induced growth of GaN NWs on Si(111) by molecular beam epitaxy (MBE). First, no Ga droplet is detected at the NW top by electron microscopy imaging,[7,8,14,16,17] so the self-catalytic effect cannot explain their formation according to the VLS mode. Second, the self-induced approach commonly employs specific MBE growth conditions: A highly nitrogen-rich vapor phase is required and often combined with a high substrate temperature.[8,17,32] Decreasing the nitrogen to gallium flux ratio often leads to a more pronounced radial growth.[8] Surface diffusion plays a crucial role in the NW elongation at the growth stage.[7,15] Third, GaN never nucleates in the NW morphology.[4,13,16–19] Rather, the nanostructures emerge as three-dimensional (3D) nanoislands having a fixed shape and a complex free surface composed of high-index atomic planes, which can be interpolated by a curved spherical cap (SC) surface.[17] In a LML case, 3D nanoislands undergo a series of shape transformations, whereby the misfit dislocations are developed at the interface prior to the NW formation.[16] After that, the full pyramid islands grow with a fixed aspect ratio before their transformation to NWs. It can therefore be concluded that NWs are relaxed from the very beginning.[13,16] During growth on an AL (where the epitaxial constraint should be very weak) the SC islands transform directly to NWs.[17] This growth transformation occurs at a critical radius of about 5 nm.[17] Fourth, GaN NWs are hexahedral, restricted by six equivalent *m*-plane vertical sidewalls[7,8,17] that are the low-energy planes. Fifth, self-induced GaN NWs usually grow in both vertical and radial directions.[7,8,15]

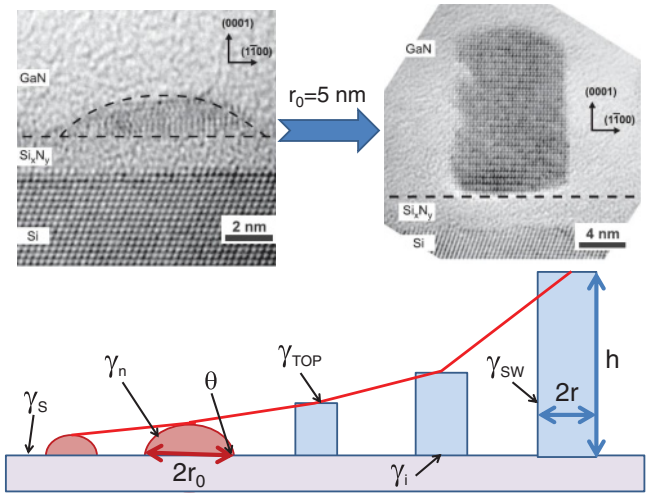

FIG. 1. (Color online) Cross-sectional view transmission electron microscopy (TEM) images of GaN SC islands and NWs on a Si_xN_y AL demonstrating the shape transformation at the SC base radius of 5 nm (top) (Ref. 17); model schematics illustrating the parameters used and the NW growth anisotropy (bottom). The shape transformation occurs instantaneously at a given volume so that the NW radius r decreases with respect to r_0.

II. SCALING GROWTH LAW

Based on the above observations, 3D nanoislands (e.g., the SC islands) grow at a fixed aspect ratio. In contrast, the aspect ratio of NWs should increase as they grow, otherwise they would not become NWs. This is the main idea of our approach. We will therefore distinguish between the two major modes of self-induced growth: (i) isotropic growth with a fixed shape, the case of quantum dots,[30,31] nanoneedles,[33] and GaN 3D islands at the initial nucleation step;[16] and (ii) anisotropic growth with the aspect ratio increasing with time, the case of GaN NWs.[7,15] The illustrations of the two growth modes, along with the data of Ref. 17 on the SC-to-NW shape transformation on an AL, are presented in Fig. 1. GaN NWs described in Ref. 17 were obtained by plasma-assisted MBE on Si(111) substrates covered by a 2-nm-thick Si_xN_y AL. The substrate temperature was kept constant at 780 °C, the nominal nitrogen and gallium rates were fixed to 2.8 and 0.45 Å/s, respectively, while the growth duration was varied.

In the foregoing analysis, we ignore the strain induced by the lattice mismatch, which is directly applicable on an AL.[17] While the energetically preferred island shape can drastically depend on the elastic relaxation and plastic deformation,[16,26] our approach would also apply to the growth on a LML, because the strain is released prior to the NW formation[13,16] and the elastically relaxed islands have a fixed pyramidal shape.[16] We consider the shape transformations due to the anisotropy of surface energies,[17] which must be the dominant driving force for any self-induced growth in the absence of lattice mismatch. We then couple this with the above-mentioned NW growth anisotropy in order to access different growth scenarios. Likewise in Refs. 29–31, our thermodynamic approach is based on the comparison of the formation enthalpies of a 3D island and a NW having the same volume under identical growth conditions. The driving force for the island-to-NW shape transformation is defined by the difference of the corresponding formation enthalpies. The kinetic volume term $\Delta\mu V$ (where $\Delta\mu$ is the difference of chemical potentials in the metastable phase and in the solid state and $V = \text{const}$ is the volume) should be identical in strain-free islands and NWs[26] and cancels in the driving force. It is therefore sufficient to consider only the surface and edge contributions (surface energy for brevity).

We now assume the scaling dependence of the NW height on its radius

$$h = \nu r^{\alpha}, \tag{1}$$

where ν is a constant and α is the growth index. The case of $\alpha = 1$ relates to an isotropic growth; the islands elongate with time at $\alpha > 1$ (the NW case where the vertical growth is faster than the radial extension) and flatten at $\alpha < 1$. Equation (1) expresses the evolution of a given NW and does not contradict the well-known relation $h \sim 1/r$ characteristic for the diffusion-induced growth,[7] which describes an ensemble of NWs at a given moment in time. By analyzing TEM and scanning electron microscopy (SEM) images of our NWs grown at typical MBE conditions with different growth durations, the length – radius dependence can thoroughly be deduced.[34] The NW length and radius were assessed among a population of more than 50 NWs, taking into account both the incubation and the transition time that are needed before the NW growth starts, and the coalescence effects at a later growth stage. As seen from Fig. 2, the averaged $h(r)$ curve remarkably follows the scaling Eq. (1) with $\alpha = 2.46$ and $\nu = 0.14$ in the particular MBE growth experiment.

III. MODEL

The volume of a 3D island growing in an isotropic mode is given by $V_{\text{isl}} = k_V r_0^3$, where k_V is a shape constant and r_0 is the base radius. In particular, $k_V = [\pi f(\theta)]/3$ with $f(\theta) = [(1 - \cos\theta)(2 + \cos\theta)]/[(1 + \cos\theta)\sin\theta]$ in the case of SC islands with the contact angle θ (see Fig. 1). The volume of a hexahedral NW with side r and height h writes as $V_{\text{NW}} = (3\sqrt{3}/2)r^2h$. From the condition $V_{\text{isl}} = V_{\text{NW}}$ and Eq. (1), one

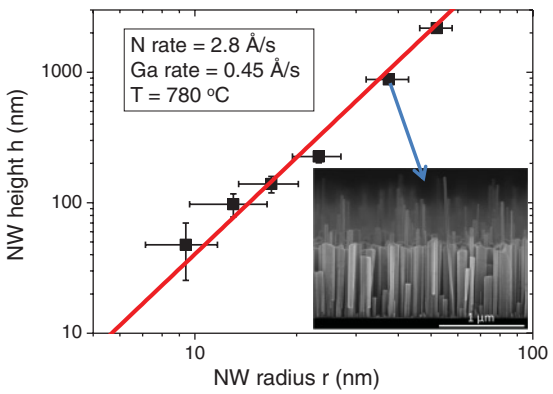

FIG. 2. (Color online) Superlinear dependence $h = 0.14r^{2.46}$ (line), obtained as the best fit to the results of statistical analyses of TEM and SEM images of GaN NWs on an amorphous interlayer (dots). A typical cross-sectional view SEM image is shown in the insert.

obtains

$$r_0 = \left(\frac{3\sqrt{3}v}{2k_V}\right)^{1/3} r^{\frac{2+\alpha}{3}}. \quad (2)$$

The surface energy generated upon the formation of a 3D island can be generally put in the form

$$G_{\rm isl} = \left(\sum_n k_n\gamma_n + k_i(\gamma_i - \gamma_S)\right) r_0^2 + k_\varepsilon \varepsilon_{\rm isl} r_0. \quad (3)$$

Here, γ_n are the surface energies of planes terminating the island surface, γ_i is the interfacial energy, γ_S is the surface energy of the substrate, and $\varepsilon_{\rm isl}$ is the specific edge energy of the island,[30] with k being the shape constants. For example, $\sum_n k_n\gamma_n = 2\pi\gamma_{\rm SC}/(1+\cos\theta)$, $k_i = \pi$, and $k_\varepsilon = 2\pi$ for the SC islands, in which $\gamma_{\rm SC}$ is the corresponding surface energy.[17] The surface energy of a hexahedral NW of radius r and height h is given by

$$G_{\rm NW} = 6\gamma_{\rm SW} rh + \frac{3\sqrt{3}}{2}(\gamma_{\rm top} + \gamma_i - \gamma_S)r^2 + 6\varepsilon_{\rm NW} r, \quad (4)$$

with $\gamma_{\rm SW}$ as the sidewall surface energy, $\gamma_{\rm top}$ as the surface energy of the top facet, and $\varepsilon_{\rm NW}$ as the specific edge energy of the NW.

Expressing r_0 through r in Eq. (3) by means of Eq. (2) and rearranging different terms, we arrive at

$$g_\alpha(r) = br^{\frac{\alpha-1}{3}} + cr^{-\frac{2(\alpha-1)}{3}} + dr^{-\frac{(2\alpha+1)}{3}} - er^{-\frac{(\alpha+2)}{3}} - 1. \quad (5)$$

Here, $g_\alpha(r) = (G_{\rm NW} - G_{\rm isl})/(Ar^{2(2+\alpha)/3})$ is the normalized difference of surface energies. The superlinear NW growth is preferred at $g_\alpha(r) < 0$ and suppressed at $g_\alpha(r) > 0$. The coefficients are defined as follows:

$$b = B/A,\ \ c = C/A,\ \ d = D/A,\ \ e = E/A, \quad (6)$$

where

$$A = \left(\frac{3\sqrt{3}v}{2k_V}\right)^{2/3}\left(\sum_n k_n\gamma_n + k_i(\gamma_i - \gamma_S)\right),$$
$$B = 6v\gamma_{\rm SW},\ \ C = \frac{3\sqrt{3}}{2}(\gamma_{\rm top} + \gamma_i - \gamma_S), \quad (7)$$
$$D = 6\varepsilon_{\rm NW},\ \ E = \left(\frac{3\sqrt{3}v}{2k_V}\right)^{1/3} k_\varepsilon\varepsilon_{\rm isl}.$$

The analysis of the driving force given by Eq. (5) simplifies with neglect of the edge terms. Since the latter are short ranged, such an analysis remains qualitatively correct in the general case. At $d = e = 0$, the function $g_\alpha(r)$ is negative between the two critical radii $r_{1,2} = x_{1,2}^{3/(\alpha-1)}$, where $x_{1,2}$ are the positive roots of the cubic equation

$$bx^3 - x^2 + c = 0. \quad (8)$$

The two roots exist provided that

$$b^2 c < 4/27. \quad (9)$$

This inequality should be treated as the necessary condition for any self-induced anisotropic growth driven by the surface energetics and starting from 3D islands. It is noteworthy that Eq. (9) is much more sensitive to the sidewall energy b than to the in-plane energy c.

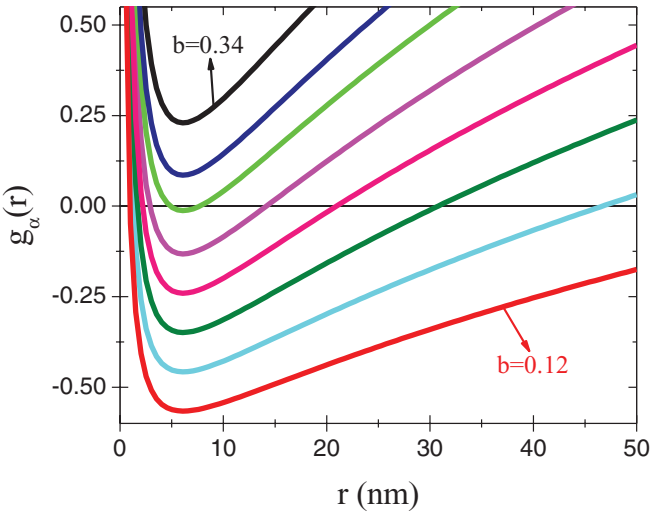

FIG. 3. (Color online) Graphs of $g_\alpha(r)$ obtained from Eq. (5) with different b decreasing from 0.34 to 0.12 at fixed $c/b = 7$ and $d = e = 0$.

Graphs of the driving force for a hypothetical model system at $\alpha = 2.46$, $v = 0.14$, fixed $c/b = 7$, zero edge terms and different b are presented in Fig. 3. The curves demonstrate a very strong dependence of the system performance on b. With the sidewall surface energy coefficient decreasing from 0.34 to 0.12, the energetically preferred NW region in r extends from zero to a wide range between ~1 and ~75 nm. The critical radius r_1 of the island-to-NW shape transformation decreases from 5 to 1 nm as the b_α decreases from 0.273 to 0.12. It should be noted that the existence of the maximum dimension for the energetically preferred anisotropic growth is inevitable in our quasiequilibrium model, since the b term in Eq. (5) increases infinitely at large r for any $\alpha > 1$. However, such transformations are most probably kinetically forbidden since they require a rearrangement of too many atoms. Also, sufficiently thick NWs may coalesce due to their high surface density,[16] which makes the second critical radius r_2 physically unreachable (at $r_2 \gg r_1$).

As discussed, the driving force given by Eq. (5) applies whenever the volume contribution into the formation enthalpy is identical for the islands and NWs, while the NW height-radius dependence is given by the scaling Eq. (1). The scaling index α as well as the surface energies defining the coefficients in Eq. (5) may depend on the growth kinetic effects. In this sense, our model treats the driving force for the energetically preferred NW formation in a particular growth experiment. A detailed study of NW growth kinetics enabling the determination of α at the given growth conditions is presented in Ref. 34. We note, however, that the energetic tendency for the island-to-NW shape transformation will be preserved in a certain domain of radii for any $\alpha > 1$ provided that the inequality (9) is satisfied, i.e., at a low enough surface energy of NW sidewalls. Indeed, the condition for the preferred anisotropic NW growth given by Eq. (9) does not depend on α at all, while its dependence on v cancels in view of Eqs. (7). This feature is illustrated in Fig. 4, where the driving force is plotted against the NW radius at fixed $b = 0.21$, $c = 1.47$, zero edge contributions, and different α. It is seen that the

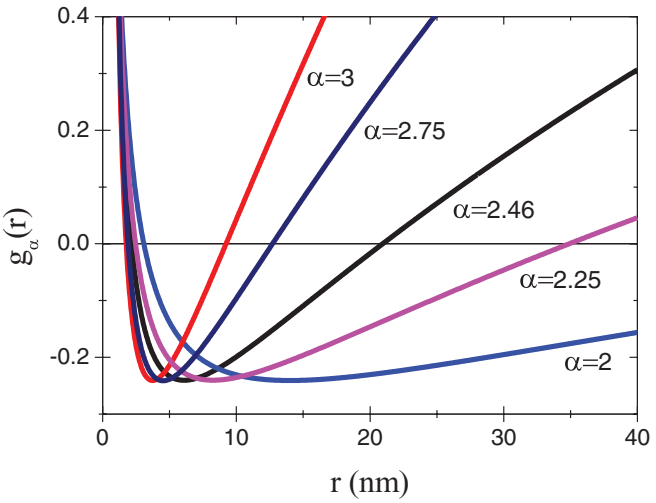

FIG. 4. (Color online) Driving force for the island-to-NW shape transformation at different α.

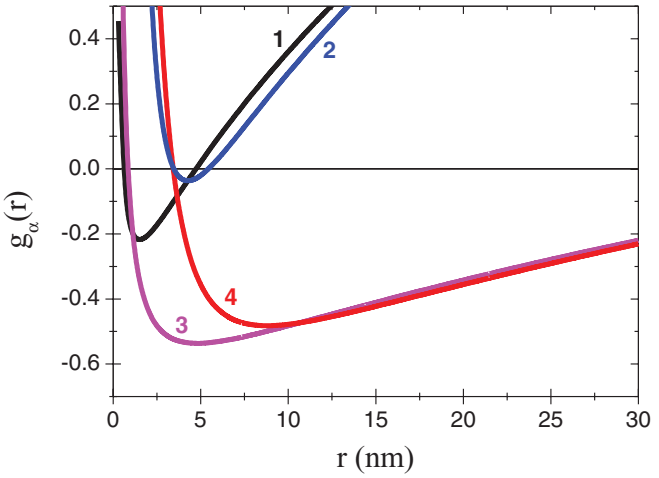

FIG. 5. (Color online) Driving forces for the superlinear NW growth at $\alpha = 2.46$ and $\nu = 0.14$ for different parameters of GaN on an AL.

first critical radius does not change significantly, while the energetically preferred NW region extends drastically as the scaling index decreases from 3 to 2.

IV. RESULTS AND DISCUSSION

Let us now consider the parameters of GaN NWs on an AL corresponding to well-defined experimental growth conditions.[17] As shown in Fig. 1, the island-to-NW transformation in this case typically occurs at $r_0 = 5$ nm, relating to the first critical radius of NW $r_1 = 3.4$ nm by Eq. (2). As for the surface energies, only the values of γ_{SW} for the sidewall m planes of 118 meV/Å^2 (with neglect of surface reconstruction)[35] and $\gamma_S = 137$ meV/Å^2 (Ref. 36) are known with reasonable accuracy. We therefore study the driving force given by Eqs. (5)–(7) within a plausible range of surface energies, sticking to the experimental scaling indices deduced from the data of Fig. 2.

We first use the values given in Ref. 17: $\gamma_i = 40$ meV/Å^2 by the analogy with the Si/SiO_2 interface, and $\gamma_{SC} = 130$–176 meV/Å^2 from the Young's equation. The surface energy of the NW top facet must be larger than γ_{SW}, because the nucleation-mediated vertical growth (involving the formation of m-plane facets of a monolayer height) is faster than the radial one (involving the formation of c planes). We therefore use the value of γ_{top} between 120 and 130 meV/Å^2. With the experimental contact angle of the spherical cap islands $\theta = 42^\circ$,[17] and the scaling parameters $\alpha = 2.46$ and $\nu = 0.14$ (also extracted from our MBE experiments), this yields the following average values of coefficients: $A = 228$, $B = 99$, $C = 86$, $b = 0.43$, and $c = 0.38$. The corresponding driving force with zero edge terms is shown in Fig. 5 (curve 1). It is seen that the energetically preferred NW region is quite narrow, extending from 1 to 5 nm only. Curve 2 in Fig. 5 corresponds to the same surface energies with the edge contributions at $d = 12$ and $e = 6$. Inclusion of the edge terms corrects the critical radius r_1 of the shape transformation to the experimental value of 3.4 nm, but the NW region remains narrow. However, we definitely observe a thermodynamic tendency for the NW formation in the correct range of critical radii.

Further, the value of interfacial energy γ_i at 40 meV/Å^2 might be largely underestimated, because the GaN/Si_xN_y interface should be much more energetic than the Si/SiO_2. This argument should hold since GaN and Si_xN_y materials form a heterogeneous interface, which is distinctly different from the Si/SiO_2 homogeneous interface. We therefore use the value of $\gamma_i = 150$ meV/Å^2 as the upmost estimate. Since the dangling bonds of m-plane sidewalls can be passivated by N under nitrogen-rich conditions, we take the value of $\gamma_{SW} = 90$ meV/Å^2 as the lowest estimate. The SC island surface is composed of high-index atomic planes of high surface energy, and many edges separating the planes, which may result in a much higher surface energy γ_{SC} than that given in Ref. 17. We thus use the value of $\gamma_{SC} = 200$ meV/Å^2 as the upmost estimate. With this parameter set, the coefficients entering Eq. (5) are changed to $A = 526$, $B = 76$, $C = 372$, $b = 0.144$, and $c = 0.71$, the case relating to the widest range of energetically preferred GaN NW growth on an AL. The corresponding driving force at $d = e = 0$ is given by curve 3 in Fig. 5. As in the previous case, the curve without the edge terms predicts a lower critical radius r_1 ($\cong$1 nm), while the curve with the edge terms corrects it to the experimental value. This corresponds to curve 4 in Fig. 5 obtained with $d = 14$ and $e = 4.5$. While nothing can be said about the edge energy, it usually increases with the inclination angle of island facets.[30] In view of a small ν in Eq. (7) for E, the inequality $d > e$ (obtained for both limit cases considered) seems reasonable. The edge terms are thus shown to be important at the beginning of growth, in particular, for the determination of the first critical radius. Otherwise, the two curves match at large r, showing that the second critical radius r_2 for the reverse transformation to an isotropic mode is determined entirely by the surface energies.

As mentioned already, the surface energies of GaN NW facets are sensitive to the vapor environment in a particular growth experiment, while the scaling index α may depend on the kinetic factors. The results shown in Figs. 4 and 5 demonstrate that the value of r_1 is not considerably affected by varying these values. This yields the island-to-NW shape

transformation within a plausible range of parameters. We note, however, that the scaling growth law given by Eq. (1) with $\alpha > 1$ is absolutely necessary to explain why GaN tends to nucleate in the form of Volmer-Weber islands rather than NWs at the beginning of growth, and undergoes the shape transformation only when the base dimension exceeds a certain critical value. Indeed, at $\alpha = 1$ Eq. (5) with zero edge terms becomes radius independent, $g_1 = b + c - 1$, showing that, while one of isotropic geometries might be preferred to another, no critical radius for the shape transformation exists in the isotropic case. Hence, the anisotropy of surface energies must be coupled with the scaling growth anisotropy to observe the self-induced nucleation of NWs from preexisting islands, which is the main message of this work. On the other hand, changing the growth conditions strongly affects the r_2 value, however, the reverse transformation to an isotropic growth should be suppressed on kinetic grounds. It can therefore be said that the initial stage of NW nucleation is driven by the surface energetics in a wide range of deposition conditions, while the followup NW growth itself proceeds in the kinetically controlled mode.

To conclude, whenever the condition for the anisotropic growth given by Eq. (9) is fulfilled, the model predicts two distinct stages of system evolution for $\alpha > 1$: (i) *Nucleation and isotropic growth of islands at* $r < r_1$. Since $g_\alpha(r) > 0$ at small r, the nanostructures cannot nucleate as NWs. Rather, they emerge as nanoislands and then grow according to an isotropic mode. At a certain time, the base dimension hits the first critical radius at which Δg_α becomes zero. This eventually leads to the development of straight NW sidewalls and starts the growth anisotropy. Since the shape transformation occurs almost instantaneously, the base dimension discontinuously decreases and the height discontinuously increases at the transition point. This can result in an overlap between SC and NW sizes for the critical radius as suggested by the experimental data in Ref. 17. (ii) *Anisotropic NW growth* is preferred between r_1 and r_2, because the growth anisotropy decreases the surface energy at a given volume. The NW height increases faster than the radius as given by Eq. (1). Anisotropic elongation again becomes more energetically costly than isotropic growth at $r = r_2$, since, at this time, the increase of sidewall surface area outweighs their low energy in the overall energy balance. However, kinetic limitations should prevent this second transformation, which, to the best of our knowledge, has not been observed experimentally.

We now plan to consider in more detail the nucleation barriers of differently shaped islands on a LML by taking into account the elastic relaxation and plastic deformation.[16,26] We will study in more detail the kinetics of self-induced NW growth at different deposition conditions such as the temperature and Ga flux. In particular, it would be very important to identify the kinetic tuning knobs that can be used to tailor the properties of self-induced GaN NWs, for example, by changing the scaling growth indices.

ACKNOWLEDGMENTS

This work was partially supported by different scientific programs of the Russian Academy of Sciences, grants of the Russian Foundation for Basic Research (Grants No. 10-02-00847-a, No. 10-02-93107-a, No. 11-02-12011-ofi-m-2011, No. 11-02-12152-ofi-m-2011, and No. 12-02-91162-a), contracts with the Russian Ministry of Education and Science No. 16.740.11.0019, No. 14.740.11.0898, and No. 16.740.11.0019, the FP7 projects SOBONA (Contract No. 268154) and FUNPROB (Contract No. 269169), as well as by the German BMBF joint research project MONALISA (Contract No. 01BL0810).

*dubrovskii@mail.ioffe.ru

[1] Y. Li, J. Xiang, F. Qian, S. Gradecak, Y. Wu, H. Yan, D. A. Blom, and C. M. Lieber, Nano Lett. **6**, 1468 (2006).
[2] S. Gradecak, F. Qian, Y. Li, H. G. Park, and C. M. Lieber, Appl. Phys. Lett. **87**, 173111 (2005).
[3] O. Hayden, G. F. Zheng, P. Agarwal, and C. M. Lieber, Small **3**, 2048 (2007).
[4] M. Yoshizawa, A. Kikuchi, M. Mori, N. Fujita, and K. Kishino, Jpn. J. Appl. Phys. **36**, L459 (1997).
[5] M. A. Sanchez-Garcia, E. Calleja, E. Monroy, F. J. Sanchez, F. Calle, E. Muñoz, and R. Beresford, J. Cryst. Growth **183**, 23 (1998).
[6] M. Wolz, V. M. Kaganer, O. Brandt, L. Geelhaar, and H. Riechert, Appl. Phys. Lett. **98**, 261907 (2011).
[7] R. K. Debnath, R. Meijers, T. Richter, T. Stoica, R. Calarco, and H. Lüth, Appl. Phys. Lett. **90**, 123117 (2007).
[8] M. Tchernycheva, C. Sartel, G. Cirlin, L. Travers, G. Patriarche, J. C. Harmand, Le Si Dang, J. Renard, B. Gayral, L. Nevou, and F. Julien, Nanotechnology **18**, 385306 (2007).
[9] R. Calarco, R. Meijers, R. K. Debnath, T. Stoica, E. Sutter, and H. Lüth, Nano Lett. **7**, 2248 (2007).
[10] A. Bertness, A. Roshko, L. M. Mansfield, T. E. Harvey, and N. A. Sanford, J. Cryst. Growth **300**, 94 (2007).
[11] T. Stoica, E. Sutter, R. J. Meijers, R. K. Debnath, R. Calarco, H. Lüth, and D. Grützmacher, Small **4**, 751 (2008).
[12] H. W. Seo, Q. Y. Chen, L. W. Tu, C. L. Hsiao, M. N. Iliev, and W. K. Chu, Phys. Rev. B **71**, 235314 (2005).
[13] O. Landre, C. Bougerol, H. Renevier, and B. Daudin, Nanotechnology **20**, 415602 (2009).
[14] R. Songmuang, T. Ben, B. Daudin, D. Gonzalez, and E. Monroy, Nanotechnology **21**, 295605 (2010).
[15] E. Galopin, L. Largeau, G. Patriarche, L. Travers, F. Glas, and J. C. Harmand, Nanotechnology **22**, 245606 (2011).
[16] V. Consonni, M. Knelangen, L. Geelhaar, A. Trampert, and H. Riechert, Phys. Rev. B **81**, 085310 (2010).
[17] V. Consonni, M. Hanke, M. Knelangen, L. Geelhaar, A. Trampert, and H. Riechert, Phys. Rev. B **83**, 035310 (2011).
[18] C. Chèze, L. Geelhaar, A. Trampert, and H. Riechert, Appl. Phys. Lett. **97**, 043101 (2010).
[19] V. Consonni, A. Trampert, L. Geelhaar, and H. Riechert, Appl. Phys. Lett. **99**, 033102 (2011).
[20] C. Chèze, L. Geelhaar, O. Brandt, W. Weber, H. Riechert, S. Münch, R. Rothemund, S. Reitzenstein, A. Forchel, T. Kehagias,

P. Komninou, G. P. Dimitrakopulos, and T. Karakostas, Nano Res. **3**, 528 (2010).
[21]A. I. Persson, M. W. Larsson, S. Stengstrom, B. J. Ohlsson, L. Samuelson, and L. R. Wallenberg, Nat. Mater. **3**, 677 (2004).
[22]F. Glas, J. C. Harmand, and G. Patriarche, Phys. Rev. Lett. **99**, 146101 (2007).
[23]V. G. Dubrovskii, G. E. Cirlin, N. V. Sibirev, F. Jabeen, J. C. Harmand, and P. Werner, Nano Lett. **11**, 1247 (2011).
[24]J. B. Hannon, S. Kodambaka, F. M. Ross, and R. M. Tromp, Nature (London) **440**, 69 (2006).
[25]L. Rigutti, G. Jacopin, L. Largeau, E. Galopin, A. D. Bugallo, F. H. Julien, J. C. Harmand, F. Glas, and M. Tchernycheva, Phys. Rev. B **83**, 155320 (2011).
[26]X. Zhang, V. G. Dubrovskii, N. V. Sibirev, and X. Ren, Cryst. Growth Des. **11**, 5441 (2011).
[27]W. Guo, A. Banerjee, P. Bhattacharya, and B. S. Ooi, Appl. Phys. Lett. **98**, 193102 (2011).
[28]V. G. Dubrovskii, N. V. Sibirev, G. E. Cirlin, A. D. Bouravleuv, Yu. B. Samsonenko, D. L. Dheeraj, H. L. Zhou, C. Sartel, J. C. Harmand, G. Patriarche, and F. Glas, Phys. Rev. B **80**, 205305 (2009).
[29]J. Tersoff and R. M. Tromp, Phys. Rev. Lett. **70**, 2782 (1993).
[30]V. A. Shchukin, N. N. Ledentsov, P. S. Kop'ev, and D. Bimberg, Phys. Rev. Lett. **75**, 2968 (1995).
[31]V. G. Dubrovskii and N. V. Sibirev, Phys. Rev. B **77**, 035414 (2008).
[32]S. Fernández-Garrido, J. Grandal, E. Calleja, M. A. Sánchez-García, and D. López-Romero, J. Appl. Phys. **106**, 126102 (2009).
[33]M. Moewe, L. C. Chuang, S. Crankshaw, C. Chase, and C. Chang-Hasnain, Appl. Phys. Lett. **93**, 023116 (2008).
[34]V. G. Dubrovskii, V. Consonni, L. Geelhaar, A. Trampert, and H. Riechert, Appl. Phys. Lett. **100**, 153101 (2012).
[35]J. E. Northrup and J. Neugebauer, Phys. Rev. B **53**, R10477 (1996).
[36]J. C. Idrobo, H. Iddir, S. Ögüt, A. Ziegler, N. D. Browning, and R. O. Ritchie, Phys. Rev. B **72**, 241301(R) (2005).